ChemComm

COMMUNICATION

View Article Online
View Journal | View Issue

Cite this: *Chem. Commun.*, 2025, **61**, 5309

Received 23rd December 2024,
Accepted 25th February 2025

DOI: 10.1039/d4cc06612j

rsc.li/chemcomm

Toward predicting silver ion binding in proteins†

A. Bianchi,[a] F. Marquenet,[a] L. Manciocchi,[b] M. Spichty[b] and K. M. Fromm*[a]

The binding of metal ions in proteins is often crucial for their function and hence for life. Silver is known to possess antimicrobial properties, yet little is known about the exact molecular mechanism of action. Based on the silver binding tetrapeptide moieties HX_1X_2M, and MX_1X_2H found in the silver efflux pump protein SilE, we studied the influence of the individual amino acids X_1 and X_2 and found trends that may be important in general metal ion binding in proteins.

Silver has been used for many years in *e.g.* jewellery, silverware and cell staining, as well as in medicine. Silver nanoparticles and ions are known to possess antimicrobial properties.[1–4] In bacteria, silver ions interfere with biomolecules causing their alteration, such as DNA condensation, production of reactive oxygen species, or protein damage.[5,6] Due to its manyfold targets in the cell, its exact mechanism of action remains unknown. Gram-negative bacteria *Salmonella Typhimurium* are able to tolerate larger amounts of silver than other bacteria by expressing a silver efflux system Sil, encoded on a transferable plasmid pMG101.[7–10] This silver efflux system is similar in protein number and function to the copper efflux system Cus, except for one specific protein, SilE, which had initially been proposed to bind up to five Ag^+.[7] In a more recent study, it has been suggested to bind eight Ag^+.[11]

SilE is a small periplasmic protein composed of 143 amino acids (aa), the first twenty of which are cleaved after periplasmic targeting (Fig. 1).[12] In contrast to metal ion binding metallothioneins, SilE does not contain cysteine, but a striking number of histidine (His, H) and methionine (Met, M) residues, organized mainly in tetrapeptide (and one tripeptide) entities, which could be expected to bind Ag^+ ions (Fig. 1).[12–14]

In previous model studies in our group, Chabert *et al.* highlighted that each HX_nM (n = 1, 2) peptide was able to coordinate to one Ag^+.[14] The affinity constants, $\log(K_{ass})$, varied between 5.3 and 6.6 (Fig. 1), indicating a moderate effect of the non-binding aa X found in between His and Met.[14]

Based on these observations and to gain a more basic understanding of how the directly silver binding moieties His and Met, as well as the different aa in between, are affecting the binding of metal ions (*e.g.*, Ag^+) in proteins, and thus able to predict the behaviour of the binding sites in proteins, simple tetrapeptide models HX_1X_2H, MX_1X_2M, HX_1X_2M, and MX_1X_2H inspired by SilE were synthesized and studied (Table 1).

All synthesized tetrapeptides were protected at the N-terminal by acetylation, and at the C-terminal by amidation (see ESI†).[15] The aa ($X_{1,2}$) in between the binding His and Met were selected according to their side chain properties at pH 7.4. We chose the positively charged arginine (Arg, R) and lysine (Lys, K), the polar uncharged glutamine (Gln, Q), the hydrophobic alanine (Ala, A), and the turn inducer proline (Pro, P). These

Model	$\log(K_{ass})$	Model	$\log(K_{ass})$
HQM	5.6 ± 0.1	MNEH	5.4 ± 0.1
MDQH	5.8 ± 0.1	HEFM	6.6 ± 0.1
HETM	6.4 ± 0.1	HQAM	5.9 ± 0.1
HQKM	5.7 ± 0.1	HRRM	5.3 ± 0.1
HQRM	5.5 ± 0.1		

Fig. 1 The SilE protein sequence is composed of 143 a.a. The twenty-first a.a. (green) correspond to the signal peptide. The nine His and Met containing motifs (underlined in black) were studied by Chabert *et al.* and inspired the library of simple tetrapeptide models used in this work, which featured motifs such as HX_1X_2H, MX_1X_2M, HX_1X_2M, and MX_1X_2H. In addition, the affinity constants below the SilE protein sequence were highlighted by Chabert *et al.*[12,14]

[a] *Univ. Fribourg, Department of Chemistry and National Center of Competence in Research Bio-inspired Materials, Chemin du Musée 9, 1700 Fribourg, Switzerland. E-mail: katharina.fromm@unifr.ch*

[b] *Univ. Strasbourg/Univ. Haute-Alsace, Laboratoire d'Innovation Moléculaire et Applications, Rue Alfred Werner 3 bis, 68057 Mulhouse Cedex, France*

† Electronic supplementary information (ESI) available: Experimental details, binding constant determination, ESI-MS spectra. See DOI: **https://doi.org/10.1039/d4cc06612j**

Table 1 Binding constants (log(K_{ass})) found by fluorimetry competition titration of a solution of tetrapeptide with the HEWM probe (1 equivalent) in MOPS buffer (20 equivalent, pH 7.4–7.5) by addition of $AgNO_3$ solution (0 to 2.6 equivalent), at 25 °C. (a) HXXM and MXXH tetrapeptide motifs. (b) HXXH and MXXM tetrapeptide motifs

a	Model	log(K_{ass})	Model	log(K_{ass})	b	Model	log(K_{ass})	Model	log(K_{ass})
Gln/Q & Arg/R	HQQM	5.6 ± 0.1	MQQH	5.5 ± 0.1	Gln/Q & Arg/R	HQQH	6.0 ± 0.1	MQQM	—
	HRQM	5.4 ± 0.1	MRQH	5.2 ± 0.1		HRQH	5.8 ± 0.1	MRQM	5.1 ± 0.1
	HQRM	5.5 ± 0.2	MQRH	5.1 ± 0.2		HQRH	5.8 ± 0.1	MQRM	5.1 ± 0.1
	HRRM	5.3 ± 0.1	MRRH	5.2 ± 0.1		HRRH	5.5 ± 0.1	MRRM	5.0 ± 0.2
Pro/P & Gln/Q	HPPM	5.0 ± 0.2	MPPH	5.1 ± 0.1	Pro/P & Gln/Q	HPPH	5.7 ± 0.1	MPPM	4.9 ± 0.1
	HQPM	5.5 ± 0.1	MQPH	5.5 ± 0.2		HQPH	6.0 ± 0.1	MQPM	4.9 ± 0.1
	HPQM	5.5 ± 0.1	MPQH	5.6 ± 0.1		HPQH	5.7 ± 0.1	MPQM	5.0 ± 0.1
	HQQM	5.6 ± 0.1	MQQH	5.5 ± 0.1		HQQH	6.0 ± 0.1	MQQM	—
Lys/K & Arg/R	HKKM	5.2 ± 0.1	MKKH	5.0 ± 0.2	Lys/K & Arg/R	HKKH	5.6 ± 0.1	MKKM	4.8 ± 0.2
	HRKM	5.2 ± 0.1	MRKH	5.1 ± 0.1		HRKH	5.4 ± 0.1	MRKM	4.9 ± 0.2
	HKRM	5.3 ± 0.1	MKRH	5.2 ± 0.1		HKRH	5.6 ± 0.1	MKRM	4.9 ± 0.1
	HRRM	5.3 ± 0.1	MRRH	5.2 ± 0.1		HRRH	5.5 ± 0.1	MRRM	5.0 ± 0.2
Ala/A & Arg/R	HAAM	5.7 ± 0.1	MAAH	5.4 ± 0.1	Ala/A & Arg/R	HAAH	6.0 ± 0.1	MAAM	5.2 ± 0.1
	HRAM	5.5 ± 0.1	MRAH	5.3 ± 0.1		HRAH	5.8 ± 0.1	MRAM	4.9 ± 0.1
	HARM	5.6 ± 0.1	MARH	5.3 ± 0.1		HARH	5.8 ± 0.1	MARM	5.1 ± 0.2
	HRRM	5.3 ± 0.1	MRRH	5.2 ± 0.1		HRRH	5.5 ± 0.1	MRRM	5.0 ± 0.2

five aa were selected because they all occur naturally in the SilE, and because of their side-chain diversity at physiological pH.

Electrospray ionization mass spectrometry (ESI-MS) confirmed in all cases that the tetrapeptide was synthesized (Fig. S58–S112, ESI†) and formed a 1 : 1 complex in the presence of Ag^+ that is stable over time (Fig. S113, ESI†). This confirms the trend observed by Chabert *et al.* who used ^{1}H NMR titrations for other previously studied peptides and their coordination to Ag^+.[14,16]

From circular dichroism (CD), it can be concluded that all tetrapeptides possess a flexible random coil structure (Fig. 2a). Upon Ag^+ addition, the CD spectra of most tetrapeptides do not indicate strong changes or a trend to fold into an α-helix (Fig. S114 and S115, ESI†), confirming that our tetrapeptides are likely too short and flexible to form a stable H-bond on $O_i \rightarrow N_{i+4}$, which is characteristic of the α-helix.[17] Only MPQH and HQPH showed a clearer trend towards a helix formation.

To determine the log(K_{ass}) of each tetrapeptide towards Ag^+, we chose fluorometric competition titration experiments (Fig. S116–225, ESI†), using the previously developed tetrapeptide HEWM as a competitor probe (Fig. 2b).[20] The best buffer system to use for titration experiments of biomolecules with Ag^+ was found to be 3-(*N*-morpholino)propanesulfonic acid (MOPS).[16,21] The tryptophan in HEWM absorbs at 280 nm and emits at *ca.* 360 nm. The log(K_{ass}) of the probe had been determined to be 6.4 ± 0.2.[16] Fluorometric competition titrations showed fluorescence quenching upon Ag^+ binding (Fig. 2c). All fluorescence intensity maxima were reported and plotted against the ratio [Ag^+]/([tetrapeptide] + [HEWM]), and DynaFit software generated a fitting curve yielding the log(K_{ass}) (Fig. 2d).[18,19]

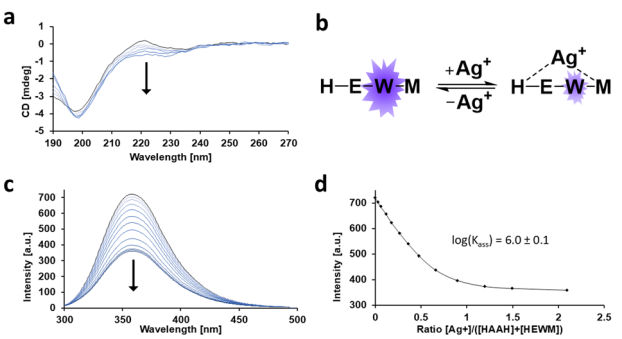

Fig. 2 (a) CD titration of HQQH (1×10^{-5} M) by addition of $AgNO_3$ (0 to 8 equivalent) at 25 °C. (b) Operating principle of the fluorescent HEWM probe. (c) HQQH (5×10^{-6} M) fluorimetry competition titration with the HEWM probe (5×10^{-6} M) in MOPS buffer (20 equivalents, pH 7.4–7.5) by addition of $AgNO_3$ (0 to 2.6 equivalents) at 25 °C. (d) Plot of the maxima of (c). The solid line corresponds to the fit obtained using DynaFit software.[18,19]

The log(K_{ass}) for the HX_1X_2M and MX_1X_2H tetrapeptide library (Table 1a) show certain clear trends:

(1) The order of silver binding moieties, HX_1X_2M and MX_1X_2H, does not hugely influence the coordination as the log(K_{ass}) are very similar in the large majority of cases (*e.g.*, resp. equal at 5.2 ± 0.1 and 5.1 ± 0.1 for HRKM and MRKH). An exception to this rule is the pair HAAM and MAAH with a difference of 0.3 in $\log_{10}(K_{ass})$. The reason for this observation might be related to the His tautomerism. Binding affinity calculations based on all-atom simulations with newly developed parameters for silver(I) indicate the same value of $\log_{10}(K_{ass,HSE})$ for the two peptides HAAM and MAAH.[22] The HSE subscript indicates a microscopic affinity for the Nε–H tautomer of the neutral His side chain; Nε–H is the strongly preferred Ag^+-binding tautomer according to experiments on peptides.[14,23] According to constant pH-simulation of the apo form, however, the MAAH peptide displays a significantly decreased population of the preferred Nε–H tautomer (36%) with respect to HAAM (60%) (Table S1, ESI†). Thus, there is a larger tautomeric penalty to overcome for MAAH than for HAAM. As a result, the calculated log(K_{ass}) with tautomeric correction log($K_{ass,corr}$) is 0.22 lower for MAAH (5.47) than for HAAM (5.69), which is in agreement with the experiment (resp. 5.4 ± 0.1 and 5.7 ± 0.1 for MAAH and HAAM).

(2) The order of X_1 and X_2 also does not seem to play a crucial role in the final log(K_{ass}). This indicates that for the selected aa X_1 and X_2, there is no significant interaction of any of the side chains with His or Met (5.3 ± 0.1 for MRAH and MARH).

(3) However, if $X_1 = X_2$, different values of the $\log(K_{ass})$ depending on the nature of the a.a. X are observed. Three cases can be differentiated here: (3a) the $\log(K_{ass})$ are the least affected by the uncharged side chains (Gln and Ala) (*e.g.*, resp. equal at 5.6 ± 0.1 and 5.7 ± 0.1 for HQQM and HAAM). The length and size of the uncharged side chains do not modify the $\log(K_{ass})$ significantly. (3b) In cases where two identical positively charged aa are placed between H and M, the $\log(K_{ass})$ are decreasing significantly, *i.e.* by up to 0.5 in log-values (*e.g.*, resp. equal at 5.7 ± 0.1 and 5.2 ± 0.1 for HAAM and HKKM). This can be understood as, at physiological pH, the positively charged side chains contribute to a repulsion for the positively charged Ag^+ as the latter is coordinated by H and M. This charge effect also indicates that there is no stabilizing interaction between Ag^+ and the Lys side chains. This contrasts with the results of some previous studies which show that the Lys alone has a good stabilizing effect with Ag^+.[24,25] The length and composition of the positively charged side groups of $X_{1,2}$ do not hugely influence the $\log(K_{ass})$ (*e.g.*, resp. 5.2 ± 0.1 and 5.3 ± 0.1 for HKKM and HRRM). (3c) Surprisingly low $\log(K_{ass})$ values are observed if two Pro moieties are placed between the coordinating aa. Being a neutral aa, Pro is known to induce specific turns in peptides and proteins.[26,27] This relative rigidity of the peptide backbone could, in the case of two Pro moieties, lead to an overall less favourable conformation or tautomer to coordinate to the Ag^+ appropriately, thus explaining the small $\log(K_{ass})$ values for HPPM and MPPH motifs (resp. 5.0 ± 0.2 and 5.1 ± 0.1). CD spectra prove that no conformational changes occur upon Ag^+ addition.

To elucidate if the double Pro induces some particular geometries that disfavour Ag^+ binding or reduce the fraction of the Ag^+-favoured HSE tautomer, we performed all-atom simulations. Indeed, the fraction of the HSE tautomer, χ_{HSE}, of HAAM is increased with respect to HPPM (60% and 32%, resp., Fig. 3b and d) which leads to a larger tautomeric penalty for the latter peptide ($\Delta\log(\chi_{HSE}) = -0.3$) (see ESI†). However, the tautomeric penalty cannot fully explain the experimental low $\log(K_{ass})$ of HPPM because the calculated microscopic binding constant of the HSE tautomer increases ($\Delta\log(K_{ass,HSE}) = +0.3$) due to favorable interaction with backbone oxygen atoms (Fig. 3a and c). Thus, HPPM features actually the same calculated macroscopic binding constant as HAAM (see ESI†). Prolines are notoriously difficult systems to treat by simulations due to sampling problems (*e.g. cis*/*trans*-isomerization). We tested eventual sampling problems of the backbone by means of parallel-tempering replica exchange simulations without any effect on $K_{ass,HSE}$ (data not shown). In addition, we tested the impact of *cis*-Pro isomerization on the affinity: $K_{ass,HSE}$ is even larger for all-*cis* or single-*cis* HPPM than for all-*trans* HPPM. Thus, the disagreement between simulations and experiments remains an open question. The answer to this might be an integrative approach for the binding affinity calculations that combines constant-pH simulations with enhanced sampling techniques to target simultaneously His tautomerism, *cis*–*trans* isomerism, and rigorous conformational sampling; this is reserved for future work.

Furthermore, we simulated MPQH (apo/holo) (Fig. 3e) *via* MD to explore the impact of Ag^+ on 3D structure (see ESI†).

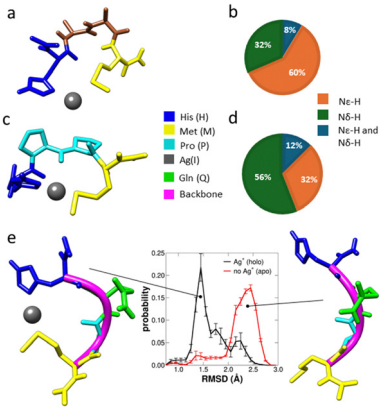

Fig. 3 (a) Most populated holo-HAAM cluster: His (blue), Met (yellow), Ala (brown), and Ag^+ (gray). (b) Apo-HAAM tautomer percentages: Nε–H tautomer (orange), Nδ–H tautomer (green) and Nε–H and Nδ–H (dark blue). (c) Most populated holo-HPPM cluster: His (blue), Met (yellow), Pro (cyan), and Ag^+ (gray). (d) Apo-HPPM tautomer percentages: Nε–H tautomer (orange), Nδ–H tautomer (green) and Nε–H and Nδ–H (dark blue). (e) The graph shows the simulated α-helix similarity of peptide MPQH without (red) and with (black) Ag^+. The probability density function of the root-mean-square deviation (RMSD) of the peptide backbone for a perfect α-helix. The smaller the RMSD, the closer the backbone conformation resembles an α-helix. Representative holo (left) and apo (right) structures are included.

The presence of Ag^+ shifts backbone conformations toward α-helices, in agreement with the CD spectrum (Fig. S115o, ESI†).

(4) For $X_1 \neq X_2$, a combination of a neutral aa with a positively charged one decreases the $\log(K_{ass})$, but to a lesser extent than if two positively charged aa are used (*e.g.*, resp. 5.6 ± 0.1 and 5.3 ± 0.1 for HARM and HKRM). Conversely, pairing a neutral aa with a negatively charged one leads to higher $\log(K_{ass})$ (*e.g.*, resp. 5.5 ± 0.1 and 5.8 ± 0.1 for MQQH and MDQH (Fig. 1)). As before, this can be explained by the fact that the side chains attract or repel more the positively charged Ag^+. Interestingly, the $\log(K_{ass})$ is not reduced with only one Pro found in either position X_1 or X_2, compared to motifs without any Pro (*e.g.*, 5.5 ± 0.1–0.2 for MQQH and MQPH). Hence, it can be concluded that a single Pro moiety does not reduce the backbone flexibility enough to lead to lower $\log(K_{ass})$.

To confirm that the side chain length does not affect the $\log(K_{ass})$, two artificial aa (Aaa) were introduced in the H-Aaa-QM motif. The first one, 2-aminohexanoic acid, Hex, has a four carbon side chain, while the second one, 2,3-diamino propanoic acid, Dap, has an ammonium function at the end of a one-carbon side chain. Comparing HAQM and H-Hex-QM, it is evident that increasing the length of the side chain does not affect the constant (both equal 5.6 ± 0.1). Similarly, for HKQM and H-Dap-QM, decreasing the length of the side chain does not play a crucial role in $\log(K_{ass})$ (resp. 5.3 ± 0.1 and 5.5 ± 0.1).

In the second part of the study, we wanted to explore the trends occurring in HX_1X_2H and MX_1X_2M tetrapeptides (Table 1b). In analogy to the previous tetrapeptides, HX_1X_2H and MX_1X_2M were synthesized and analyzed. Despite many attempts to modify the synthesis and purification protocols, the MQQM tetrapeptide remained trapped in the filter due to its hydrophobic nature and could not be properly studied.

Comparing the log(K_{ass}) of this new HX_1X_2H and MX_1X_2M tetrapeptide library (Table 1b) shows that, like for HX_1X_2M and MX_1X_2H, the positions of X_1 and X_2 do not seem to affect the affinity constants (*e.g.*, 5.8 ± 0.1 for HRQH and HQRH). Like before, uncharged side groups do not seem to influence the log(K_{ass}) (*e.g.*, 6.0 ± 0.1 for HQQH and HAAH), independently of their size, while charged aa in position X_1 and/or X_2 reduce the log(K_{ass}). The effect, and hence the lowering of the log(K_{ass}) value, is approximately the same for HX_1X_2H and MX_1X_2M.

From a general perspective, trends show that HQQH, HAAH, and HQPH tetrapeptides have the larger log(K_{ass}) value in this series with 6.0 ± 0.1. On the other hand, MKKM has the smallest value with 4.8 ± 0.2, meaning that Ag^+ prefers to bind with HQQH, HAAH, or HQPH over MKKM by a factor of 15.8. This confirms our previous observation that HX_1X_2H tetrapeptides have higher values, and MX_1X_2M have lower ones, and also that positively charged side chains lead to lower log(K_{ass}) values than uncharged side chains. Furthermore, a very clear trend is that the log(K_{ass}) of HX_1X_2H is always higher than that of HX_1X_2M or MX_1X_2H, and also much higher than that of MX_1X_2M tetrapeptide (*e.g.*, log(K_{ass}) of HKRH > HKRM ≈ HKRM > MKRM). According to the hard–soft acid–base (HSAB) theory, Ag^+, considered as a soft Lewis acid, would bind more easily to the sulfur atom in Met than to the nitrogen atom in His.[28] However, both literature and experiments show the opposite.[14,16,29] Indeed, the relative silver(I) ion binding energies for His (18.0 ± 0.1 kcal mol^{-1}), and Met (13.1 ± 0.1 kcal mol^{-1}) indicate that Ag^+ prefers to be coordinated by His rather than Met.[30]

Additionally, it should be noted that introducing a second Pro moiety between two His and two Met residues results in a less significant reduction of the log(K_{ass}) compared to the HX_1X_2M and MX_1X_2H tetrapeptides. The differences between HPQH/HPPH or MPQM/MPPM are roughly 0.1, while the differences between HPQM/HPPM or MPQH/MPPH are more significant, *i.e.* 0.5.

Finally, the log(K_{ass}) of HX_1X_2M and MX_1X_2H can be roughly predicted by the following mathematical equation: $\log(K_{HXXM}) \approx \log(K_{MXXH}) = (\log(K_{HXXH}) + \log(K_{MXXM}))/2$. For example, the theoretical log(K_{ass}) of HQPM is 5.6, which is quite close to the experimental value of 5.5 ± 0.1. For HARM, both values are identical, *i.e.* 5.6.

In conclusion, this work highlights a library of log(K_{ass}) for Ag^+-tetrapeptide complexes by using short model peptides inspired by SilE protein. The log(K_{ass}) were determined through fluorometric competition titrations with the HEWM probe in MOPS buffer by the addition of $AgNO_3$ solution. This provides a more fundamental understanding of which aa are particularly prone to influencing the binding of Ag^+ in proteins in general. Their affinity range ($10^{4.8}$–$10^{6.0}$) reveals that the nature of the non-binding aa (X_1 and X_2) seems to moderately affect the log(K_{ass}) between Ag^+ and tetrapeptide. Additionally, this work marks an initial and crucial step toward predicting the behaviour of metal ion binding sites within proteins. This might be important for metal ion chaperones that transfer metal ions from one protein to another, just as much as in proteins of multiple binding sites to predict sequential binding and conformational changes. We will therefore continue our studies of SilE and its models to elucidate more details of its coordination to Ag^+.

K. M. F. provided the initial idea, won competitive funding, and supervised the entire project. A. B. was responsible for the synthesis and analysis of most of the tetrapeptides. F. M. synthesized and analyzed some tetrapeptides as part of his doctoral research. Simulations were conducted by L. M. and M. S. K. M. F., A. B., L. M., and M. S. participated in the writing and review of the final version of this communication. All authors approved the content and submission.

The authors thank the University of Fribourg, Fribourg Center for Nanomaterials, Swiss National Science Foundation (Project 2000020_172777 and 2000020 _204215), University of Strasbourg (Project g2023a142c/g and g2024a236c/g), and University of the Upper Alsace for generous support.

Data availability

The data supporting this article have been included as part of the ESI.†

Conflicts of interest

There are no conflicts to declare.

Notes and references

1 D. J. Barillo and D. E. Marx, *Burns*, 2014, **40**, S3.
2 I. Chopra, *J. Antimicrob. Chemother.*, 2007, **59**, 587.
3 S. Medici, M. Peana, V. M. Nurchi and M. A. Zoroddu, *J. Med. Chem.*, 2019, **62**, 5923.
4 W. Sim, R. T. Barnard, M. A. T. Blaskovich and Z. M. Ziora, *Antibiotics*, 2018, **7**, 93.
5 S. H. Lee and B. H. Jun, *Int. J. Mol. Sci.*, 2019, **20**, S3.
6 F. Barras, L. Aussel and B. Ezraty, *Antibiotics*, 2018, **7**, 1.
7 S. Silver, *FEMS Microbiol. Rev.*, 2003, **27**, 341.
8 G. L. Mchugh, R. C. Moellering, C. C. Hopkins and M. N. Swartz, *Lancet*, 1975, **1**, 235.
9 A. Gupta, K. Matsui, J.-F. Lo and S. Silver, *Nat. Med.*, 1999, **5**, 183.
10 S. L. Percival, P. G. Bowler and D. Russell, *J. Hosp. Infect.*, 2005, **60**, 1.
11 Y. Monneau, C. Arrault, C. Duroux, M. Martin, F. Chirot, L. Mac Aleese, M. Girod, C. Comby-Zerbino, A. Hagège, O. Walker and M. Hologne, *Phys. Chem. Chem. Phys.*, 2022, **25**, 3061.
12 UniProtKB, **https://www.uniprot.org/uniprot/Q9Z4N3#**, accessed 13 May 2022.
13 D. H. Hamer, *Annu. Rev. Biochem.*, 1986, **55**, 913.
14 V. Chabert, M. Hologne, O. Sénèque, A. Crochet, O. Walker and K. M. Fromm, *Chem. Commun.*, 2017, **53**, 6105.
15 R. B. Merrifield, *J. Am. Chem. Soc.*, 1963, **85**, 2149.
16 V. Chabert, M. Hologne, O. Sénèque, O. Walker and K. M. Fromm, *Chem. Commun.*, 2018, **54**, 10419.
17 S. Narasimha and R. W. Woody, in *Circular Dichroism: Principles and Applications*, ed. N. Berova, K. Nakanishi and R. W. Woody, John Wiley & Sons, Inc., New York, 2nd edn, 2000, pp. 601–620.
18 P. Kuzmič, *Anal. Biochem.*, 1996, **273**, 260.
19 P. Kuzmič, *DynaFit (version 4.10.004)*, BioKin Ltd., Watertown, MA, 1996.
20 P. Thordarson, *Chem. Soc. Rev.*, 2011, **40**, 1305.
21 L. Babel, S. Bonnet-Gómez and K. M. Fromm, *Chemistry*, 2020, **2**, 193.
22 L. Manciocchi, A. Bianchi, V. Mazan, M. Potapov, K. Fromm and M. Spichty, *Biophysica*, 2025, **5**, 7.
23 J. L. Sudmeier, E. M. Bradshaw, K. E. Coffman Haddad, R. M. Day, C. J. Thalhauser, P. A. Bullock and W. W. Bachovchin, *J. Am. Chem. Soc.*, 2003, **125**, 8430.
24 L. Clem Gruen, *Biochim. Biophys. Acta*, 1975, **386**, 270.
25 T. Schoeib, K. W. Siu and C. Hopkinson, *J. Phys. Chem. A*, 2002, **106**, 6121.
26 A. A. Morgan and E. Rubenstein, *PLoS One*, 2013, **8**, e53785.
27 M. Levitt, *J. Mol. Biol.*, 1981, **145**, 251.
28 P. W. Ayers, *J. Chem. Phys.*, 2005, **122**, 141102.
29 G. A. Zingale, V. Oliveri and G. Grasso, *Metallomics*, 2003, **15**, 1.
30 V. W.-M. Lee, H. Li, T.-C. Lau, R. Guevremont and K. W. Michael Siu, *J. Am. Soc. Mass Spectrom.*, 1998, **9**, 760.

